

**Research Paper****Evaluation of Design Requirements for Anchor Block of Buried Pipelines****Akbar Vasseghi^{1*} and Mohammad Kermani²**

1. Associate Professor, Structural Engineering Research Center, International Institute of Earthquake Engineering and Seismology (IIEES), Tehran, Iran,

*Corresponding Author; email: vasseghi@iiees.ac.ir

2. Geotechnical Engineering Consultant, Montreal, Canada

Received: 23/01/2023**Revised:** 05/04/2023**Accepted:** 08/04/2023**ABSTRACT**

Concrete anchor blocks are usually used to restrain the axial expansion of natural gas transmission pipelines near compressor stations. Current design procedures for the anchor blocks are based on providing an adequate margin of safety against block sliding, block overturning and soil bearing pressure. This paper presents the results of an analytical study on the response of soil, pipeline and anchor block at different operating pressure and temperatures. Nonlinear finite element analyses that include modeling of soil-pipe and soil-block interactions are carried out to evaluate the design procedures. The results indicate that the concept used in current design procedures is fundamentally flawed because it is based on controlling forces rather displacements. Furthermore, both the thrust force and the resistance capacity are grossly miscalculated. The thrust force is significantly overestimated because it is based on a fully restrained anchor. The resistance capacity of the block that is calculated based on full mobilization of the passive resistance of soil is also drastically miscalculated because only a fraction of the passive resistance is mobilized.

Keywords:

Anchor block; Pipeline;
Soil-structure interaction;
Soil-pipe interaction

1. Introduction

Natural gas transmission pipelines transport the natural gas at elevated temperature and high internal pressure. For typical transmission pipelines in Iran, the normal range of operating pressure is 500-1050 psi and the normal range of temperature is 30-60 degree Centigrade. When the pipeline is put into operation, it tends to expand along its length due to the internal pressure and temperature. In buried pipelines, the pipe movement due to such expansion is fully restrained by the surrounding soil except for a relatively small length near the ends as shown in Figure (1a). The axial displacements are significant for large gas transmission pipelines. The large axial displacement may cause serious damage to equipment and structures attached to the pipeline. In order to

reduce the axial displacement, the pipeline is usually restrained near compressor stations by anchor blocks as shown in Figure (1b). Massive concrete anchor blocks are commonly used in gas transmission pipelines to resist the high thrust force resulting from the internal pressure and temperature.

The previous studies on performance and design of anchor blocks include a research by Al-Gahtani (2009) who developed a simple procedure for the optimum design of anchor blocks. He used the Rankine's theory to compute the active and passive earth pressures on the anchor block. Friction forces on sides, bottom, and top of the anchor block were taken into account by using a specific coefficient of friction between

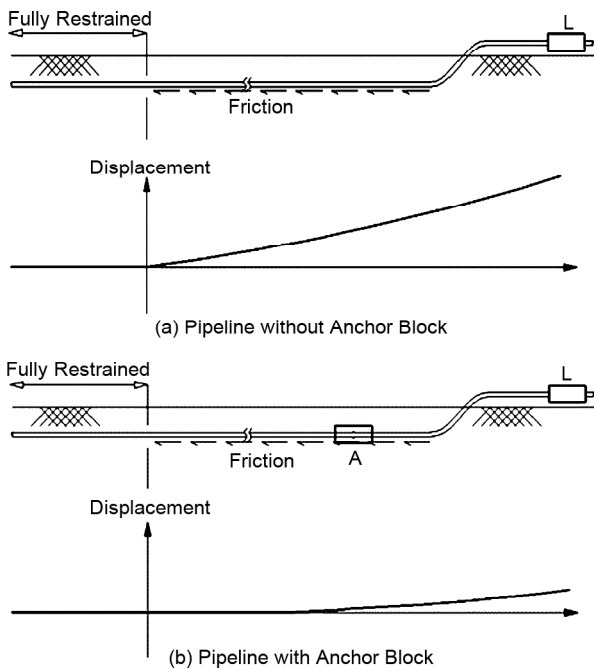


Figure 1. Axial pipeline displacement near a compressor station.

concrete and soil. Block sliding, block overturning, and soil bearing capacity were the main design parameters.

Duncan & Mokwa (2001) conducted two series of field experiments on a 900 mm × 1900 mm × 1100 mm anchor block. In this study, the calculated passive earth pressures from different theories were compared to the test results. The logarithmic spiral method with 3D correction gave the best estimate of the measured maximum passive force and the Rankine method gave a reasonable estimate of the force.

Ashrafi et al. (2019) evaluated the response of typical natural gas transmission pipelines at anchor block interface under the effect of seismic wave propagation. They performed non-linear dynamic response analysis and developed fragility functions for three typical pipelines in two types of soils. The results of this study indicate that the pipe is susceptible to local buckling failure at the pipe-anchor block interface. The results also indicate that pipeline vulnerability increases with increasing pipe diameter.

Zhang et al. (2016) proposed an analysis method to evaluate the thrust force on the anchor block using the condition of deformation compatibility and the hypothesis of stagnation point. They also performed finite element analysis for a

specific pipeline system to evaluate the accuracy of the proposed method. The results indicate that the proposed analytical method is in good agreement with the finite element results.

The performance of buried steel pipelines subjected to relative soil movements in the axial direction was investigated using full-scale pullout testing in a soil chamber by Wijewickreme et al. (2009). The test results were compared to requirements of the ASCE (1984), "Guidelines for the Seismic Design of Oil and Gas Pipeline Systems". The results showed that the guideline gave a very conservative estimate of friction force between dense sand and pipeline. For loose sand, the measured and the calculated friction forces were in a very good agreement.

The stiffness of anchor blocks resulting from the passive soil pressure is analogous to the longitudinal stiffness of bridge abutments. There are several experimental and analytical studies on bridge abutments. Wood (2009) had summarized the results of these studies. Rollins & Sparks (2002) evaluated the available experimental results and presented the test results with passive pressure versus displacements curves. Also, Stewart et al. (2007) conducted a full-scale cyclic load test on a 2600 mm × 4600 mm bridge abutment.

The objective of this paper is to evaluate the response of the anchor block when the pipeline is operated under high internal pressure and temperature. Nonlinear static finite element analyses on a 56 inch buried steel pipeline in four types of soils and various anchor blocks were carried out to evaluate the current design requirements.

2. Current Design Procedure

As temperature and internal pressure increase, the pipeline tends to expand; however, since the anchor block is assumed to fully restrain the movement of the pipe, it will resist a thrust force proportional to the amount of expansion. Based on equation proposed by Liang-Chung (1978), the thrust force that is applied to anchor block by the pipeline is calculated using Equation (1). In this equation, the term " $E\alpha(T_2 - T_1)$ " corresponds to pipeline expansion due to temperature differential ($T_2 - T_1$) and the term " $(0.5 - \nu)S_h$ " corresponds to pipeline contraction due to the Poisson's effect of

the hoop tension (S_h) resulting from the internal pressure.

$$Q = A[(0.5 - \nu)S_h + E\alpha(T_2 - T_1)] \quad (1)$$

where Q = the thrust force, ν = the Poisson's ratio, E = modulus of elasticity, A = cross sectional area of pipe, T_2 = the maximum operating temperature, T_1 = temperature at the time of installation and S_h = hoop stress due to fluid pressure.

Figure (2) shows the forces acting on the anchor block. The driving forces which tend to move the block are the trust force Q , and the force induced by active soil pressure. The active soil pressure occurs when the block moves away from the soil and the soil mass is allowed to deform outward to the point of mobilizing the soil full shear resistance. The force due to active soil pressure, F_a , is calculated using Rankin approach as per Equation (2). In this approach, it is assumed that the soil is homogeneous and isotropic, the most critical shear surface is a plane, and the block moves sufficiently to develop the active condition.

$$F_a = W \times \left[\frac{1}{2} \gamma_s H^2 K_a - 2cH \sqrt{K_a} \right] \quad (2)$$

$$K_a = (1 - \sin\phi) / (1 + \sin\phi) \quad (3)$$

where H = height of the block; W = width of the block; B = block thickness; HP = pipe centerline; c = soil cohesion; γ_s = unit weight of soil; K_a = active pressure coefficient.

The resisting forces that restrain the block from moving are due to the passive earth pressure and friction force between soil and block. The force due to the passive soil pressure, F_p , can be calculated by Equations (4) and (5).

$$F_p = W \times \left[\frac{1}{2} \gamma_s H^2 K_p + 2cH \sqrt{K_p} \right] \quad (4)$$

$$K_p = (1 + \sin\phi) / (1 - \sin\phi) \quad (5)$$

The friction along the soil-block interface may be calculated by Equation (6) (Das, 2002)

$$\tau = \sigma' \tan \delta + C'_a \quad (6)$$

where: C'_a = adhesion; and δ = effective angle of internal friction between soil and the concrete.

Therefore, the maximum bottom friction force can be calculated using Equation (7):

$$R_b = W \times B \times [\gamma_c \times H \times \tan(\delta) + C'_a] \quad (7)$$

where γ_c = unit weight of concrete.

The maximum friction force on sides of the anchor block can be derived from Equation (8).

$$R_s = B \times \left(\frac{1}{2} \times \gamma_s \times H^2 \times K_0 \times \tan \delta + H \times C'_a \right) \quad (8)$$

Finally, the total friction force can be calculated by Equation (9):

$$R_{friction} = R_b + 2R_s \quad (9)$$

Using above equations, the following design constraints are controlled in current design procedure:

1. The block must be stable against sliding. Therefore, the following equation must be satisfied:

$$\frac{R}{Q + F_a} > FS_s \quad (10)$$

where $R = FR_b + FR_s + F_p$; and FS_s is proposed to be 1.2 (Al-Gahtani, 2009).

2. The block must be stable against overturning.

Therefore, the following equation must be satisfied:

$$\frac{M_R}{M_Q} > FS_O \quad (11)$$

where M_R = the moment caused by resisting forces; and M_Q = the moment caused by thrust force and active earth pressure taken from the toe of the block. The typical recommendation for the minimum factor of safety against overturning is 1.5 (Al-Gahtani, 2009)

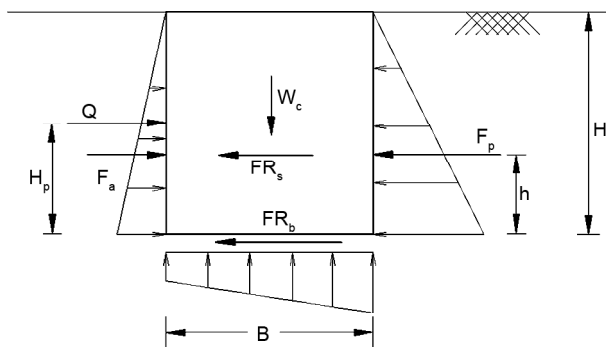


Figure 2. Forces acting on an anchor block (Al-Gahtani, 2009).

3. The largest bearing pressure is routinely at the toe of the block anchor (Lower Right corner, Figure 2). The largest bearing pressure should not exceed the allowable bearing pressure, which is usually provided by the geotechnical consultant. Therefore, Equation (12) must be satisfied:

$$0 \leq \sigma \leq q_{al} \quad (12)$$

where σ is bearing pressure and q_{al} is maximum allowable bearing pressure.

3. Analytical Study

Nonlinear static finite element analyses on a 56-inch steel pipeline was carried out using ANSYS software. The operating pressure was assumed to be 1050 psi and the temperature change was assumed to range from 0° C to 65° C. Four types of soil were considered to surround the block anchor: Dense sand, loose sand, hard clay and soft clay. The average properties of these soils are presented in Table (1).

The construction cost of the anchor block is directly proportional to the volume of the anchor block. In order to evaluate the displacement response and the safety factors, two types of anchor blocks with the same volume but with significantly different dimensions were considered in the analyses.

Anchor block type A; which was designed in accordance with the current design procedure. The factor of safety against sliding and overturning were assumed to be 1.2 and 1.5 respectively.

Anchor Block type B; which has a volume equal to block type A, width equal to one-fourth of block type A and length equal to four times length of block type A. Table (2) lists the dimensions and the design parameters of the anchor blocks. This table indicates that the factor of safety against sliding (FS_s) and maximum bearing pressures for block type B are less than block type A. However, factors of safety against overturning (FS_o) are much higher for type B blocks.

4. Finite Element Model

A nonlinear finite element model was established by using elastic pipe element to model pipeline, and nonlinear Winkler springs to model soil-pipe interaction. Preliminary analyses were performed on a 500 m long pipeline with two different mesh sizes (2.5 m and 5 m long pipe elements) to establish the model length and the appropriate mesh size. The Winkler springs representing the soil-pipe interaction were placed at end nodes of pipe elements and the analyses were performed under internal pressure of 1050 psi and temperature of 65°. These analyses indicated only marginal differences between the results of the two models

Table 1. Properties of different studied soil types.

ID	Soil Type	Unit Weight (kN/m ³)	Cohesion (kN/m ²)	Angle of Internal Friction (Degree)
1	Dense Sand	21.5	0	40
2	Stiff Clay	18.5	80	10
3	Loose Sand	18	0	18
4	Soft Clay	16.5	5	13

Table 2. Properties of different anchor blocks.

Block Type	Soil Type	Buried Depth (m)	Height (m)	Width (m)	Length (m)	FSs	FSo	Max Bearing Pressure (kN/m ²)
A	1	1.2	5.50	11.00	11.00	1.21	1.61	322.61
	2	1.2	5.50	11.80	11.00	1.22	1.73	304.17
	3	1.2	5.50	37.50	11.00	1.23	4.04	193.05
	4	1.2	5.50	45.00	11.00	1.23	4.72	181.74
B	1	1.2	5.50	2.75	44.00	0.84	5.00	195.96
	2	1.2	5.50	2.95	44.00	0.68	5.31	196.25
	3	1.2	5.50	9.38	44.00	0.91	16.00	152.00
	4	1.2	5.50	11.25	44.00	0.86	19.07	149.03

with different mesh sizes (less than 2%) indicating that model with the 5 m mesh size is adequate. The results also showed that the active length of the pipeline (the length where the pipe axial displacement diminishes to zero) is less than 400 m. Therefore, a 500 m long model with 5 m mesh size was considered to be suitable for further analyses. Nonlinear springs representing the soil-block interaction were also placed at anchor block location (Figure 3). The distance between anchor block and the pipeline end was assumed to be $b = 45$ m; and the length of the pipe above the ground level was considered as $a = 20$ m. The mechanical properties of the steel pipe are listed in Table (3).

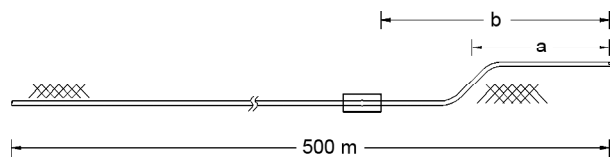


Figure 3. Finite element model.

Table 3. Properties of steel pipe used in finite element model.

Modulus of Elasticity (Mpa)	Poisson's Ratio	Linear Coefficient of Thermal Expansion ($1/^{\circ}\text{C}$)
2×10^5	0.3	11.7×10^{-6}

For the analysis, the internal pressure was initially increased from 0 to 1050 psi and then the temperature was increased from 0°C to 75°C in equal 5°C steps. The modelling parameters for soil-pipe and soil-block interactions are discussed in following sections.

4.1. Soil-Pipe Interaction Springs

The soil-pipe interaction is simulated using Winkler nonlinear discrete springs in three dimensions. The active element is the axial Elastoplastic soil spring. In accordance with the ALA 2001 and PRCI 2009 guidelines, the maximum axial spring force applied to one meter length of the pipeline can be calculated from the following equation.

$$T_u = \pi DH \gamma \frac{K_0 + 1}{2} \tan \delta \quad (13)$$

where D = pipe outside diameter; H = depth to pipe centerline; γ = effective unit weight of soil; K_0 = coefficient of pressure at rest; δ = angle of internal

friction = $f \phi$; and f = coating dependent factor relating the internal friction angle of the soil to the friction angle at the soil-pipe interface. The Guidelines for the Seismic Design of Oil and Gas Pipeline Systems (ASCE, 1984) has recommended K_0 and δ equal to 0.37 and 31° respectively for steel pipelines embedded in loose sand. These values are in compliance with results of the experimental studies carried out by Wijewickreme et al. (2009) on 18 inch steel pipe embedded in loose sand.

In accordance with the guidelines for the design of buried steel pipelines (American Lifelines Alliance, 2001), the necessary displacement for development of the maximum friction force between pipe and soil is 5 mm. Therefore, the stiffness of the longitudinal spring that is placed every 5 m on the pipe is derived from the following force-displacement values: Maximum Force = 57.9 kN and Relative Displacement = 5 mm.

4.2. Soil-Block Interaction Springs

Soil-block interaction was simulated with two nonlinear springs, one for friction force and another one for passive earth pressure (Figure 4). The maximum soil spring forces and associated displacements necessary to develop these forces must be calculated for each spring in order to estimate the stiffness of the springs.

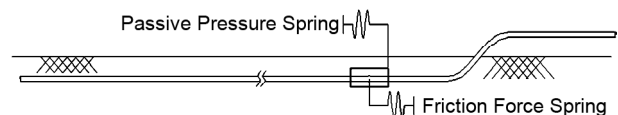


Figure 4. Finite element representation of soil-block interaction.

4.2.1. Friction Force Springs

The maximum bottom friction force can be calculated from Equation (7) and the maximum friction force on sides of the block anchor can be calculated from Equation (8). Finally, the total friction force can be calculated by Equation (9).

The maximum displacement relative to above forces is recommended in Table (4).

4.2.2. Passive Pressure Springs

The maximum passive pressure is calculated using the Equations (2) to (5). The displacement

Table 4. Displacements relative to maximum friction forces (American Lifelines Alliance, 2001).

Soil	Displacement at Maximum Friction Force (mm)
Dense Sand	3.0
Loose Sand	5.0
Stiff Clay	8.0
Soft Clay	10.0

Table 5. Typical Values of Δ_a and Δ_p (Das, 2002).

Soil Type	Δ_a/H	Δ_p/H
Loose Sand	0.001-0.002	0.01
Dense Sand	0.0005-0.001	0.005
Soft Clay	0.02	0.04
Stiff Clay	0.01	0.02

needed to fully mobilize passive and active earth pressures is presented in Table (5).

The calculated stiffness is compared with the results of the studies on bridge abutments collected by Rollins & Sparks (2002). Figure (5) shows that the values proposed by Das (2002) are in agreement with the test results. These results are also in line with equations extracted from Caltrans Seismic Design Criteria (2006).

The passive force vs. displacement curves that show the results of a field experiment conducted by Stewart et al. (2007) on a model abutment is plotted in Figure (6). The graphs resulted from Caltrans (2006), Rankin's theory and the displacement suggested by Das (2002) for dense sand are plotted to compare the theoretical calculations and experimental measurements. The Rankin's theory

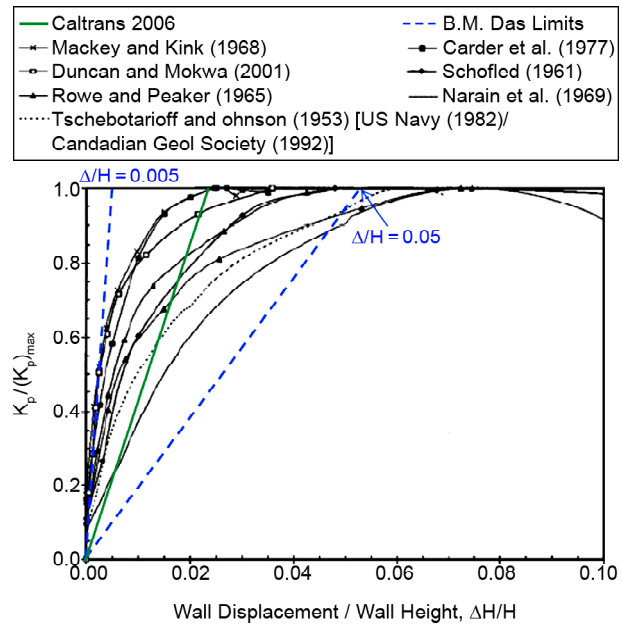


Figure 5. Relative passive earth pressure vs relative displacement for bridge abutment.

seems to be a little conservative.

In order to be able to model both active and passive pressures acting on the block, the earth pressures at the back and front of the block (passive earth pressure and active earth pressure) are simulated with one single spring, called effective passive spring. Figure (7) shows the force-displacement diagram of the effective passive spring. In this figure, Δ_a is the necessary displacement for mobilization of maximum active force and Δ_p is the necessary displacement for mobilization of maximum passive force. For block displacements less than Δ_a , the stiffness is reduced due to the

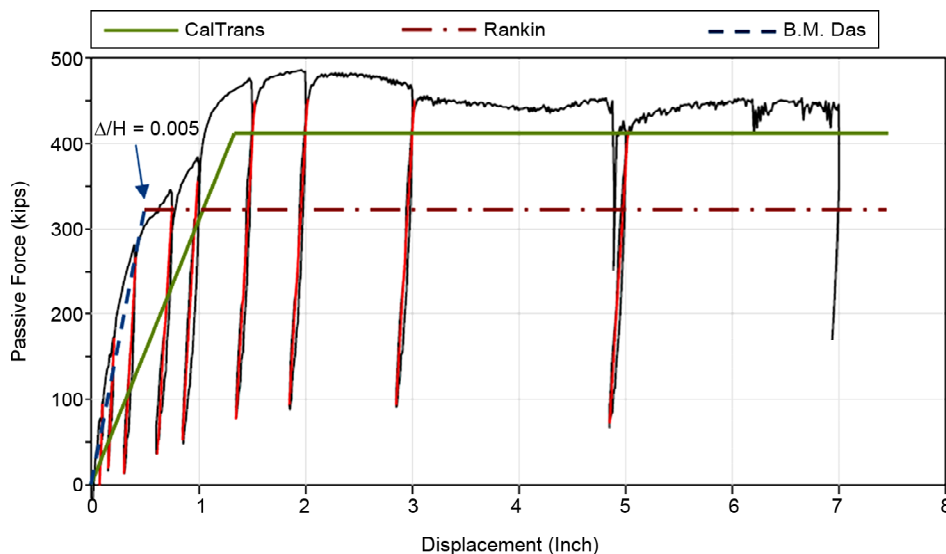


Figure 6. Passive earth pressure vs displacement for bridge abutments.

negative contribution of the active soil pressure. For block displacements greater than Δ_a , the effective force is equal to the passive force (F_p) subtracted by the active force (F_a). Table (6) lists the properties of the effective springs for different soil types and anchor blocks.

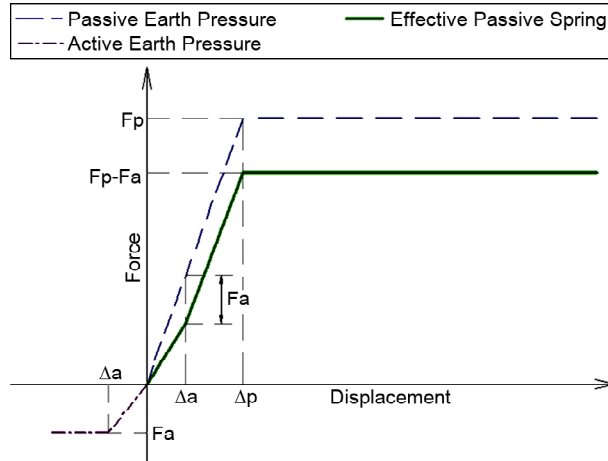


Figure 7. Force-displacement properties of effective passive spring.

5. Results of the FEM Analyses

Initially, in order to evaluate the influence of utilizing anchor block in the pipeline, no anchor block was defined in the model. Figure (8a) shows the longitudinal force and displacement response along the 56 inch pipeline under internal pressure of 1050 psi and temperature of 65°. The longitudinal displacement reaches its highest value (113 mm) at the end of the pipeline. The axial force in the pipeline reaches its highest value (15300 kN) at a distance about 300 m from the end of the pipeline. Note that this force is equal to the thrust force calculated by Equation (1) for pipe internal pressure of 1050 psi and temperature differential of 65°. To model an anchor block that completely restrains the movements of the pipeline, a fixed support in the longitudinal direction was used at the location of the anchor block. Figure (8b) shows the longitudinal force and displacement response of the pipeline with a completely

Table 6. Effective Passive Spring Properties.

Block Type	Soil Type	Block Dimensions			Friction Spring		Effective Passive Spring			
		Height (m)	Width (m)	Thickness (m)	Max Friction Force	Relative Displacement (mm)	0 < Δ < Δ _a		Δ _a < Δ < Δ _p	
							Max Force (kN)	Relative Displacement (mm)	Max Force (kN)	Relative Displacement (mm)
A	1	5.5	11.00	11	9300.4	3	2508.6	5.5	15656.9	27.5
	2	5.50	11.80	11	7787.9	8	17062.7	55	17062.7	55
	3	5.50	37.50	11	12447.1	5	2342.8	22	13943.5	55
	4	5.50	45.00	11	11840.3	10	10562.2	220	14733.4	275
B	1	5.50	2.75	44	13151.4	3	627.1	5.5	3914.2	27.5
	2	5.50	2.95	44	9570.9	8	4265.7	55	4265.7	55
	3	5.50	9.38	44	15085.4	5	585.7	22	3485.9	55
	4	5.50	11.25	44	13785.4	10	2640.5	220	3683.4	275

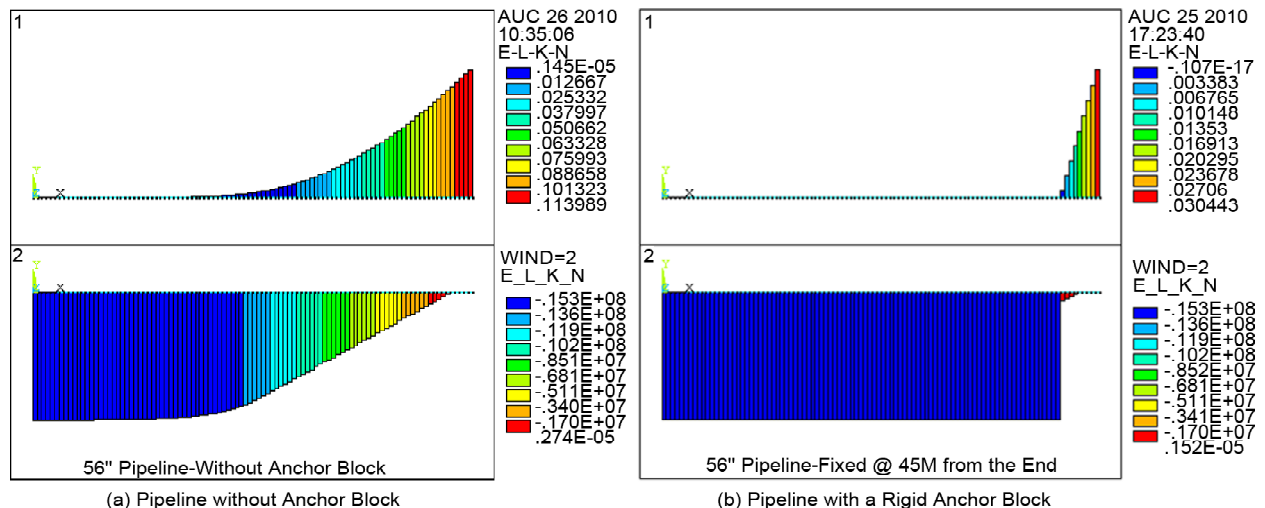


Figure 8. Force and displacement along the pipeline.

rigid anchor block. As anticipated, the rigid block totally restrains the pipeline movement at the support location and reduces the maximum longitudinal displacement at the end of the pipeline to 30 mm. This displacement due to pipeline expansion upstream of the fixed support. In this case, the pipeline thrust force of 15300 kN is totally resisted by the rigid anchor block.

5.1. Pipeline Response with Anchor Blocks Type A and B

Figure (9) shows the result of the FEM analysis for 56 inch pipeline with anchor blocks type A and B embedded in soil type 2. In both cases, there are some longitudinal displacement at the anchor block location. This displacement results in significant reduction of the thrust force resisted by the anchor block in comparison with the rigid block. This reduction is about 33% for soil type 1 and about 3 and 42% for soil types 2 and 4.

The passive, friction and total force on the block

A and B embedded in different soil types are listed in Table (7). This table also lists the maximum longitudinal displacements at the end of the pipeline, which indicated that the displacements are almost the same for the two block types. This table indicates that the total passive earth pressure would never be mobilized. The friction spring activates before passive spring because it needs smaller displacements for complete mobilization. Subsequently, as the temperature and displacement increase, the portion of the passive pressure grows. For example, for type A block in type-1 soil, while all the friction force is activated, only 20.4% of the total passive earth pressure and 50.1% of the total calculated resisting force is mobilized. Note that in ordinary design method, the whole resisting force is taken into account to calculate the factors of safety.

The forces applied to anchor block embedded in various soils in various temperatures are plotted in Figure (10). As shown in this figure, the friction

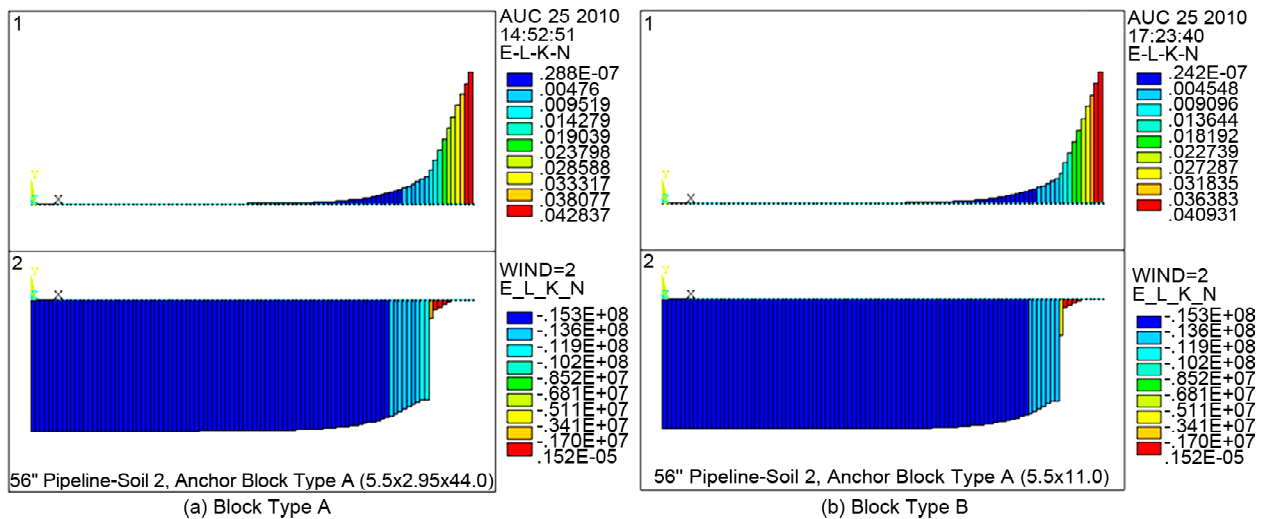


Figure 9. Force and displacement along the pipeline with anchor blocks.

Table 7. Forces and displacements in 56 inch pipeline.

Block Type	Soil Type	Force						Displacement (mm)
		Friction Force (kN)	Mobilized Friction Force (%)	Passive Force (kN)	Mobilized Passive Force (%)	Total Force (kN)	Total Mobilized Force (%)	
A	1	9300.0	100.0%	3190.7	20.4%	12490.7	50.1%	6.6
	2	7696.4	98.8%	3260.6	19.1%	10957.0	44.1%	10.5
	3	11423.5	91.8%	828.8	5.9%	12252.3	46.4%	7.8
	4	10163.4	85.8%	576.9	4.1%	10740.3	41.7%	11.8
B	1	12293.7	93.5%	704.7	18.0%	12998.4	76.2%	6.0
	2	9571.0	100.0%	963.0	22.6%	10534.0	76.1%	12.4
	3	12041.7	79.8%	460.5	13.2%	12502.2	67.3%	7.3
	4	10825.2	78.5%	150.0	4.1%	10975.2	62.8%	11.2

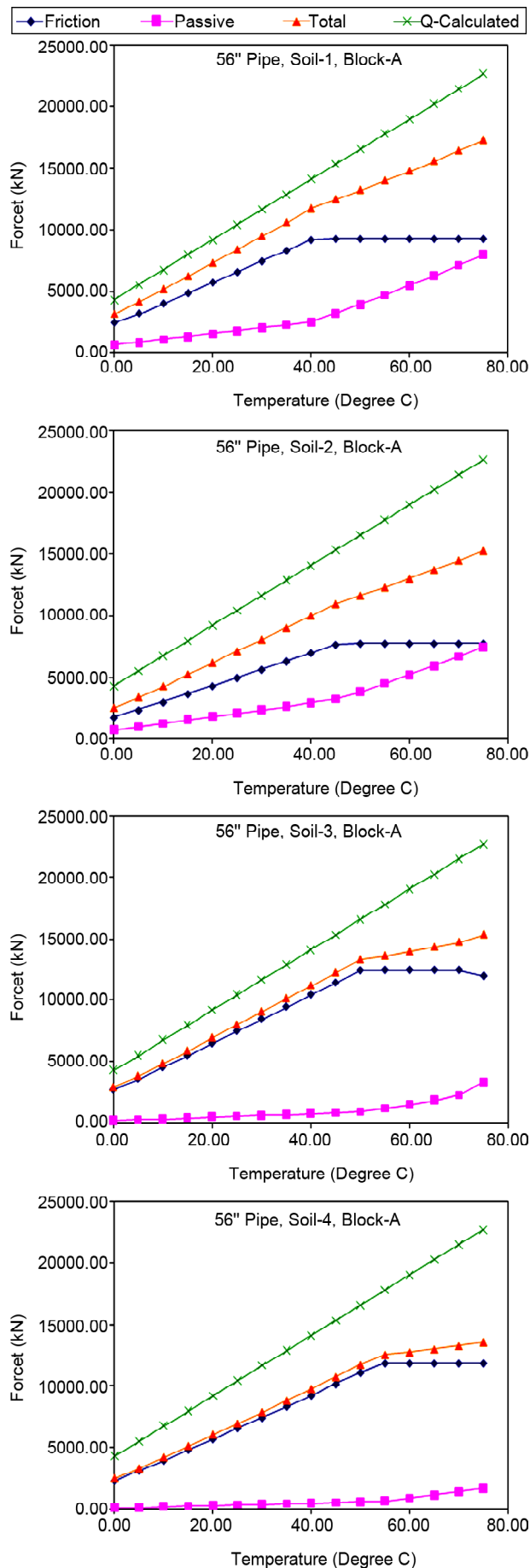


Figure 10. Forces applied to anchor block embedded in various soils vs temperature change.

spring reaches maximum force and yields at temperatures about 40°C to 50°C. As the friction spring yields, the rate of increase in maximum force with temperature decreases. It is also of interest to note that the sum of the passive spring and friction spring forces is less than the thrust force calculated by Equation (1) (i.e., Q calculated). This reduction is attributed to the displacement of the anchor block and is more pronounced in soil type 4 where the block displacement is larger than the other cases.

Passive pressure and friction forces applied to blocks type A and B embedded in different soil types are plotted in Figure (11). The friction force on block type B is higher than friction force on block type A. Inversely, the passive force on block type B is less than the passive force on block type A. Therefore, in a soil that does not have a proper passive resistance type B block may perform better.

Figure (12) shows the displacements of the anchor block embedded in different soil types. Generally, block type B moves more than block type A in soil types 1 and 2 and less than block A in soil types 3 and 4. This difference is marginal in low temperatures and is significant in high temperatures.

Figure (13) shows the displacement of the block and the end of the pipeline in different temperatures for various soil types. The movement of the end of the pipeline is significantly more than the block. This is due to the longitudinal expansion of the pipe between the block and the end of the pipeline. This length is considered to be 45 m. It is recommended to reduce this length as much as possible to prevent excessive movement of the pipeline end.

5.2. Pipeline Response with an Optimized Anchor Blocks

The results of analyses presented in the previous section clearly indicate that in soil types 3 and 4 (i.e., soft and stiff clay), the mobilized passive earth pressure is less than 6% for a typical anchor block (i.e., type A). In clayey soils where the contribution of passive soil pressure for resisting the trust force is not significant, the design of the anchor block may be optimized by relying less on the passive soil resistance and more on the frictional

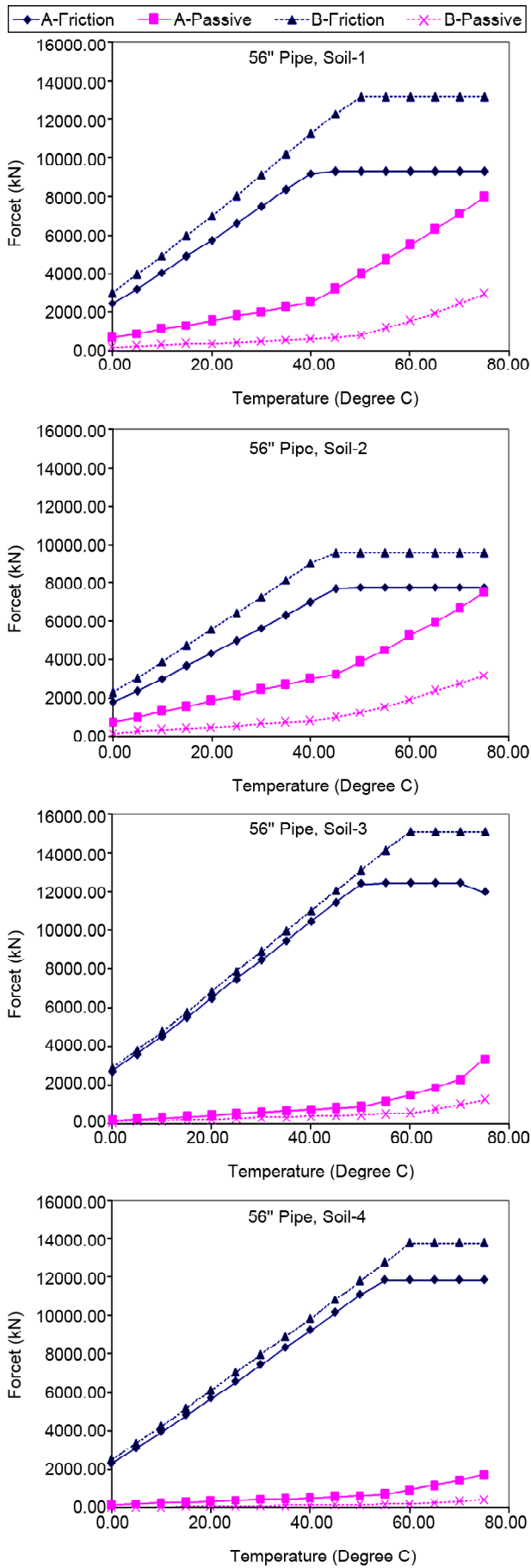


Figure 11. Block A and B forces at different pipe temperatures.

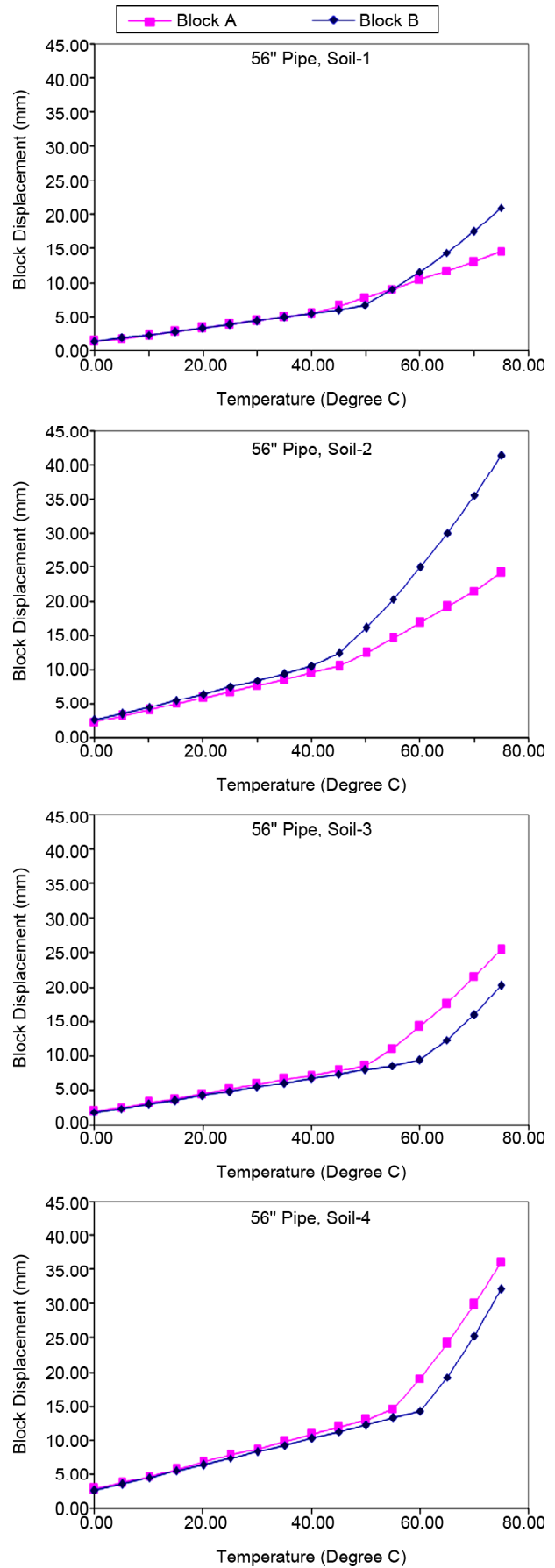


Figure 12. Block A and B displacement vs pipe temperature change.

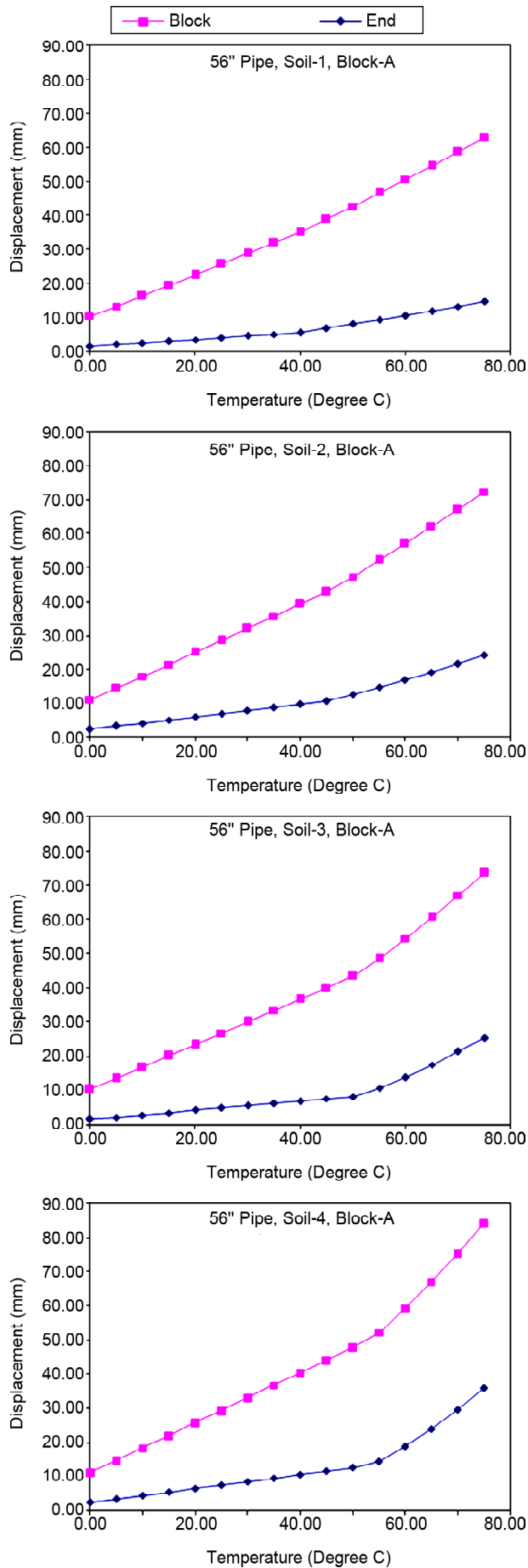


Figure 13. Block and end of pipeline movement vs temperature.

resistance. To evaluate this hypothesis, a relatively long 5.5m × 5.5m × 60m anchor block designated as type C was analyzed in type 3 soil. The properties of this anchor block are listed in Table (8). The volume of this block is 80% of that of ordinary block type A. Figure (14) shows the components of the forces applied to the anchor block type C. As shown in this figure, very little passive pressure will be mobilized in block type C and the resisting force is primarily the friction force. At 50oC temperature, all the friction force is activated, whereas the mobilized passive force is marginal.

The block displacement for type A and type C block are compared in Figure (15). At temperatures less than 70oC, the displacement of block type C is comparable to that of block type A. Figure (16) represents components of resisting force at different pipe temperatures for block type A and C. The friction force in block type C are more than block type A. On the other hand, passive earth pressure is more in block type A.

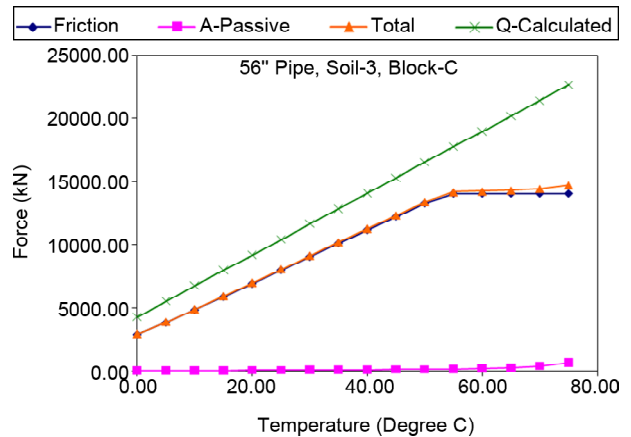


Figure 14. Forces of the anchor block type C at different pipe temperatures.

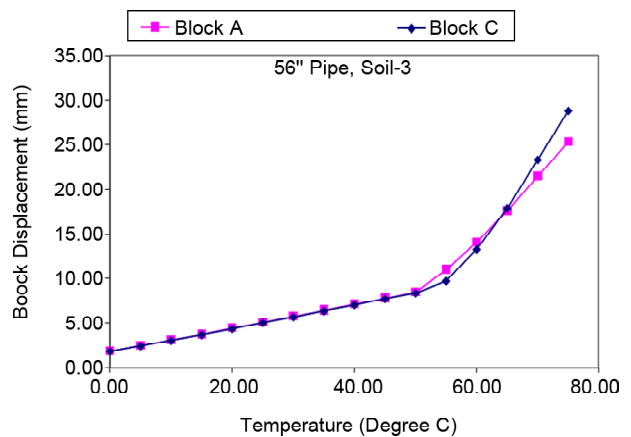


Figure 15. Block displacement vs pipe temperature for block type A and C.

Table 8. Block type C properties.

Block Type	Soil Type	Block Dimensions			Friction Spring		Effective Passive Spring			
		Height (m)	Width (m)	Thickness (m)	Max Friction Force	Relative Displacement (mm)	$0 < \Delta < \Delta_a$		$\Delta_a < \Delta < \Delta_p$	
							Max Force (kN)	Relative Displacement (mm)	Max Force (kN)	Relative Displacement (mm)
C	3	5.5	5.5	60	14051.0	5.0	343.6	22.0	2045.0	55.0

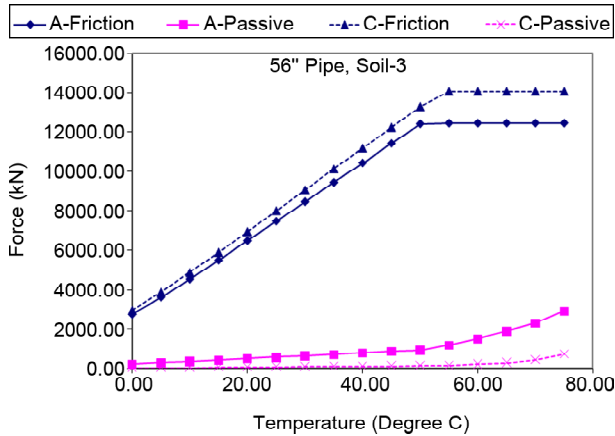


Figure 16. Friction and passive force vs pipe displacement for block type A and C.

6. Summary and Conclusions

Concrete anchor blocks are commonly used to restrain the movement of buried pipelines on both sides of compressor stations. Current design procedures for anchor blocks are usually based on providing adequate margin of safety against block sliding, block overturning and soil bearing pressure. In this study, the response of a 56-inch pipeline with three different types of anchor blocks was evaluated using finite element method. The anchor blocks designed in accordance with the current design procedures is designated as type A. Anchor block type B with the same volume as block type A has width equal to one-fourth, and length equal to four times length of block type A. Anchor block type C is a relatively long block with volume equal to 80% of block type A. Nonlinear finite element analyses was carried out to assess the response of pipeline and anchor block at different operating pressure and temperatures. The analyses were performed assuming four different soil types, i.e., dense sand (type 1), loose sand (type 2), stiff clay (type 3), and soft clay (type 4). The main results are as follows.

1. In buried pipelines without anchor blocks, the pipeline expansion takes place in a relatively

short length at the end of the pipeline. This length, which is called the active length, increases with increasing pipe diameter.

- The classic equations give a satisfactory estimate of thrust force on the anchor block if the pipeline is fully restrained. However, a small movement of the block leads to significant reduction of thrust force.
- Anchor blocks move due to the increase in pressure and temperature. Generally, block type B moves more than block type A in soil types 1 and 2 and less than block A in soil types 3 and 4. This difference is marginal in low temperatures and is significant in high temperatures.
- A large portion of the pipeline end displacement depends on the length of the unrestrained part of pipeline upstream of the anchor block. Since the pipeline end displacement is the main factor affecting the safety of the equipment attached to the pipeline, it is recommended to reduce this length as much as possible.
- The friction force and passive earth pressure are the resisting forces against thrust force. As the friction force mobilizes in smaller displacements, the contribution of this force in controlling the displacements is more than the passive force. For anchor blocks designed according to current design procedures (type A), the results of the analysis indicate that 100% of the friction force and only up to 21% of passive earth pressure would be mobilized at operating condition.
- The displacement response of the pipeline in soil type 3 with a relatively long block (type C) is comparable to that of type A block. This comparable response is achieved while the volume of block type C is 20% less than block type A.
- The current design procedures that are based on providing adequate margin of safety against block sliding and overturning is flawed because:

The thrust force is calculated assuming that the anchor block is fixed in place. The results of this study indicate that small longitudinal displacement occurs at the anchor block location. This displacement results in significant reduction of the thrust force.

The resisting force consisting of the friction and passive earth pressure are assumed to be fully mobilized. The FEM results indicate that only a fraction of the passive earth pressure will be mobilized.

Acknowledgement

The research project leading to this paper was sponsored by the Iranian Gas Engineering and Development Company (IGEDC) and it was conducted at the International Institute of Earthquake Engineering and Seismology (IIEES). The supports provided by IDEDC and IIEES are gratefully acknowledged.

References

- Al-Gahtani, H. J. (2009). Optimum design of buried pipeline block anchors. *Practice Periodical on Structural Design and Construction*. [https://doi.org/10.1061/\(asce\)1084-0680\(2009\)14:4\(190\)](https://doi.org/10.1061/(asce)1084-0680(2009)14:4(190)).
- American Lifelines Alliance (2001). *Guideline for the Design of Buried Steel Pipe*. American Society of Civil Engineers, New York, NY.
- ASCE (1984). *Guidelines for the Seismic Design of Oil and Gas Pipeline Systems*. American Society of Civil Engineers, New York, NY.
- Ashrafi, H., Vasseghi, A., Hosseini, M. & Bazli, M. (2019). Development of fragility functions for natural gas transmission pipelines at anchor block interface. *Engineering Structures*, 186, Elsevier BV. <https://doi.org/10.1016/j.engstruct.2019.02.020>.
- Caltrans (2006). *Seismic Design Criteria*. SDC-2006, California Dept. of Transportation, Sacramento, California.
- Carder, D.R., Pocock, R.G., & Murray, R.T. (1977). *Experimental Retaining Wall Facility-Lateral Stress Measurements with Sand Backfill* (No. TRRL Lab Report 766).
- Canadian Geotechnical Society (1992). *Canadian Foundation Engineering Manual*, 3rd Ed., BiTech, Vancouver, B.C., Canada.
- Das, B.M. (2002). *Principles of Geotechnical Engineering*, 5th Edition. In Brooks/Cole eBooks. <http://ndl.ethernet.edu.et/bitstream/123456789/33343/1/7.pdf>.
- Duncan, J.M. & Mokwa, R.L. (2001). Passive earth pressures: Theories and tests. *Journal of Geotechnical and Geoenvironmental Engineering*, 127(3), 248-257.
- Liang-Chung, P. (1978). *Stress Analysis Methods for Underground Pipe Lines-Part 1: Basic Calculations*. Pipe Line Industry.
- Liang-Chung, P. (1978). Stress analysis methods for underground pipe lines-part 2: soil-pipe interaction. Pipe Line Industry.
- Mackey, R.D. and Kirk, D.P. (1968). At rest, active and passive earth pressures. *Proc., Southeast Asian Conf. on Soil Mech. and Found. Engrg.*, Asian Institute of Technology, Bangkok, Thailand, 187-199.
- Narain, J., Saran, S. & Nandakumaran, P. (1969). Model study of passive pressure in sand. *Journal of the Soil Mechanics and Foundations Division*, 95(4), 969-984.
- PRCI (2009). *Pipeline Integrity for Ground Movement Hazards*. Houston: Pipeline Research Council International.
- Rollins, K.M. and Sparks, A. (2002). Lateral resistance of full-scale pile cap with gravel backfill. *Journal of Geotechnical and Geoenvironmental Engineering*, 128(9), 711-723.
- Rowe, P.W. & Peaker, K. (1965). Passive earth pressure measurements. *Geotechnique*, 15(1), 57-78.
- Schofield, A.N. (1961). The development of lateral force of sand against the vertical face of a rotating model foundation. *In Proceedings of the 5th International Conference on Soil Mechanics and Foundation Engineering*, Paris, 2, 479-494.
- Stewart, J.P., Taciroglu, E. Wallace, J.W, Ahlberg,

E.R., Lemnitzer, A., Rha, C., et al. (2007). Full scale cyclic testing of foundation support systems for highway bridges: part II: abutment backwalls. *UCLA: Civil and Environmental Engineering*.

Tschebotarioff, G.P. & Johnson, E.G. (1953). *The Effects of Restraining Boundaries on the Passive Resistance of Sand: Results of a Series of Tests with a Medium-Scale Testing Apparatus*. Report Submitted to the Office of Naval Research, Dept. of the Navy. Department of Civil Engineering, Princeton University.

Wijewickreme, D., Karimian, H., & Honegger, D.H. (2009). Response of buried steel pipelines subjected to relative axial soil movement. *Canadian Geotechnical Journal*, 46(7), 735-752. <https://doi.org/10.1139/t09-019>

Wood, J.H. (2009). Resistance from bridge abutment passive soil pressure in earthquakes. *Proceedings NZSEE Annual Conference*.

Zhang, L., Yan, X. & Yang, X. (2016). Using the unit force method to analyze thrust acting on anchor blocks caused by thermal expansion displacement of X80 tunnel pipelines. *Journal of Pipeline Systems Engineering and Practice*, 7(1). [https://doi.org/10.1061/\(asce\)ps.1949-1204.0000202](https://doi.org/10.1061/(asce)ps.1949-1204.0000202).